ELSEVIER

Tectonophysics 307 (1999) 235–254

TECTONOPHYSICS

www.elsevier.com/locate/tecto

Oceanic plateau and island arcs of southwestern Ecuador: their place in the geodynamic evolution of northwestern South America

Cédric Reynaud [a], Étienne Jaillard [a,b], Henriette Lapierre [a,*], Marc Mamberti [a,c], Georges H. Mascle [a]

[a] *UPRES, A-5025, Université Joseph Fourier, Institut Dolomieu, 15 rue Maurice-Gignoux, 38031 Grenoble cedex, France*
[b] *IRD (formerly ORSTOM), CS1, 209–213 rue La Fayette, 75480 Paris cedex 10, France*
[c] *Institut de Minéralogie et Pétrographie, Université de Lausanne, BFSH2 (3171), 1015 Lausanne, Switzerland*

Received 12 August 1997; accepted 11 March 1999

Abstract

Coastal Ecuador is made up of an oceanic igneous basement overlain by Upper Cretaceous to Lower Paleocene (≈98–60 Ma) volcaniclastic and volcanic rocks of island-arc affinities. The igneous basement, known as the Piñón Formation, locally dated at 123 Ma, consists of olivine-free basalts and dolerites. Relative to N-MORB, both types of rocks exhibit high concentrations in Nb (0.3–10.75 ppm), Ta (0.03–0.67 ppm), Th (0.11–1.44 ppm), light and medium rare earth elements, and low Zr (22–105 ppm) and Hf (0.59–2.8 ppm) contents, thus showing oceanic plateau basalts affinities. Most of these oceanic plateau basalts tholeiites display rather homogeneous $\varepsilon_{Nd\,(T=123\,Ma)}$ ratios ($\sim+7$), with the exception of two rocks with higher (+10) and lower (+4.5) $\varepsilon_{Nd\,(T=123\,Ma)}$, respectively. All these basalts plot, with one exception, within the ocean island basalts field. Their $(^{87}Sr/^{86}Sr)_i$ ratios are highly variable (0.7032–0.7048), probably due to hydrothermal oceanic alteration or assimilation of altered oceanic crust. The rocks of the Piñón Formation are geochemically similar to the oceanic plateau tholeiites from Nauru and Ontong Java Plateaus and to the Upper Cretaceous (92–88 Ma) Caribbean Oceanic Plateau lavas. The basalts and dolerites of the Upper Cretaceous–Lower Paleocene island arcs show calc-alkaline affinities. The ε_{Nd} ratios (+6.1 to +7.1) of these arc-rocks are very homogenous and fall within the range of intra-oceanic island-arc lavas. The Upper Cretaceous–Lower Paleocene calc-alkaline and tholeiitic rocks from coastal Ecuador share similar high ε_{Nd} ratios to Cretaceous intra-oceanic arc rocks from north, central and South America and from the Greater Antilles. Since the Piñón oceanic plateau tholeiites are locally overlain by early-Late Cretaceous sediments (∼98–83 Ma) and yielded locally an Early Cretaceous age, they do not belong to the Late Cretaceous Caribbean Oceanic Plateau. The basement of coastal Ecuador is interpreted as an accreted fragment of an overthickened and buoyant oceanic plateau. The different tectonic units of coastal Ecuador cannot be easily correlated with those of western Colombia, excepted the Late Cretaceous San Lorenzo and Ricaurte island arcs. It is suggested that northwestern South America consists of longitudinally discontinuous terranes, built by repeated accretionary events and significant longitudinal displacement of these terranes.

Keywords: oceanic plateau; island arc; accretion; Western Ecuador; Cretaceous–Paleocene

* Corresponding author. Tel.: +33-7687-4643; Fax: +33-7687-8243; E-mail: henrietlapierre@ujf.grenoble.fr

0040-1951/99/$ – see front matter
PII: S0040-1951(99)00099-2

1. Introduction

Subduction of oceanic plates occurred beneath the western margin of the South American continental plate since at least Early Jurassic times (e.g. James, 1971; Aspden et al., 1987; Jaillard et al., 1990). However, whereas no mafic complexes nor exotic oceanic terranes are known in central South America (Mégard, 1987), northwestern South America is characterized by the presence of mafic terranes of oceanic origin (e.g. Gansser, 1973; Toussaint and Restrepo, 1994). Recent work carried out in western Colombia has demonstrated that several accreted terranes are remnants of oceanic plateaus (Millward et al., 1984; Nivia, 1996; Kerr et al., 1996; Kerr et al., 1997a,b), the buoyancy of which may explain why they have not been subducted.

In Ecuador, a NNE-trending Late Jurassic–earliest Cretaceous ophiolitic suture has been mapped (Aspden and Litherland, 1992), which separates the crystalline basement of the Eastern Cordillera (Litherland et al., 1994) from the oceanic volcanic rocks of western Ecuador (Fig. 1). The coastal terrane was regarded as a fragment of oceanic floor (Goossens and Rose, 1973; Goossens et al., 1977; Juteau et al., 1977), overlain by intra-oceanic volcanic arcs (Lebrat et al., 1987; Jaillard et al., 1995), and accreted to the Andean margin during Late Cretaceous (Lebrat et al., 1987), Paleocene (Daly, 1989; Van Thournout et al., 1992) and/or Eocene times (Feininger and Bristow, 1980; Bourgois et al., 1990).

No detailed geochemical and isotopic studies have been carried out on the mafic rocks of coastal Ecuador, and their nature, age and origin are yet poorly constrained. The aim of this paper is to present new results on the mineralogy, petrology, geochemical and isotopic signatures of the igneous basement in coastal Ecuador. Together with recent and current geological studies (Jaillard et al., 1997; Cosma et al., 1998; Lapierre et al., 1999), the new data allow us to refine the geological evolution and geodynamic significance of this probably composite terrane, to compare its tectonic history and significance with the oceanic plateau fragments of western Colombia, and to discuss its origin.

2. Geological framework

The Piñón Formation is regarded as the Cretaceous igneous basement of western Ecuador, made up of tholeiitic basalt–andesitic pillow basalts and massive flows, locally associated with pillow-breccias, hyaloclastites and subordinate siliceous sediments. So far, it is considered as a piece of oceanic floor (Goossens and Rose, 1973; Juteau et al., 1977; Lebrat et al., 1987), that locally possesses island-arc affinities (Goossens et al., 1977; Henderson, 1979). The volcanic rocks are intruded by doleritic and/or gabbroic stocks. The studied samples come from two distinct geological domains of coastal Ecuador.

In the northwestern area (Manabí, Figs. 1 and 2), altered and metamorphosed basalt flows of N-type MORB composition, ascribed to the Piñón Formation, yielded unreliable K–Ar ages ranging from 110 to 54 Ma (Goossens and Rose, 1973). The Piñón Formation is of pre-late Campanian age ($\sim$pre-78 Ma), since it is overlain by sediments palaeontologically dated as late Campanian and cross-cut by late Campanian intrusions (Pichler and Aly, 1983; Wallrabbe-Adams, 1990). The northwestern area seems to be separated from the central area by a NE- to NNE-trending fault system running east of Manta and southeast of Esmeraldas (Fig. 1).

In the San Lorenzo area (Fig. 1), coarse-grained greywackes and volcaniclastic conglomerates associated with basaltic flows, ash beds, dikes and scarce thin limestone beds, are interpreted as resting on the Piñón Formation. These volcanic rocks, named the San Lorenzo Formation, are related to the activity of an intra-oceanic arc (Lebrat et al., 1987). Interpillow sediments of the San Lorenzo Formation are dated by late Campanian and Maastrichtian microfauna (Sigal, 1969; Faucher et al., 1971; Jaillard et al., 1995; Ordoñez, 1996). Volcanic rocks yielded K–Ar ages of 85–65 Ma (Goossens and Rose, 1973; Pichler and Aly, 1983) and an ^{40}Ar–^{39}Ar age of 72.7 ± 1.4 Ma (Lebrat et al., 1987). This succession is then unconformably overlain by fore-arc marine sediments of Middle Eocene age (Cerro, San Mateo Formations), within which the abundance of detrital quartz indicates that this area was already accreted to the continental margin (Manabí Basin, Benítez, 1995; Jaillard et al., 1995, 1997; Fig. 2).

The central area (Guayaquil area) is a little

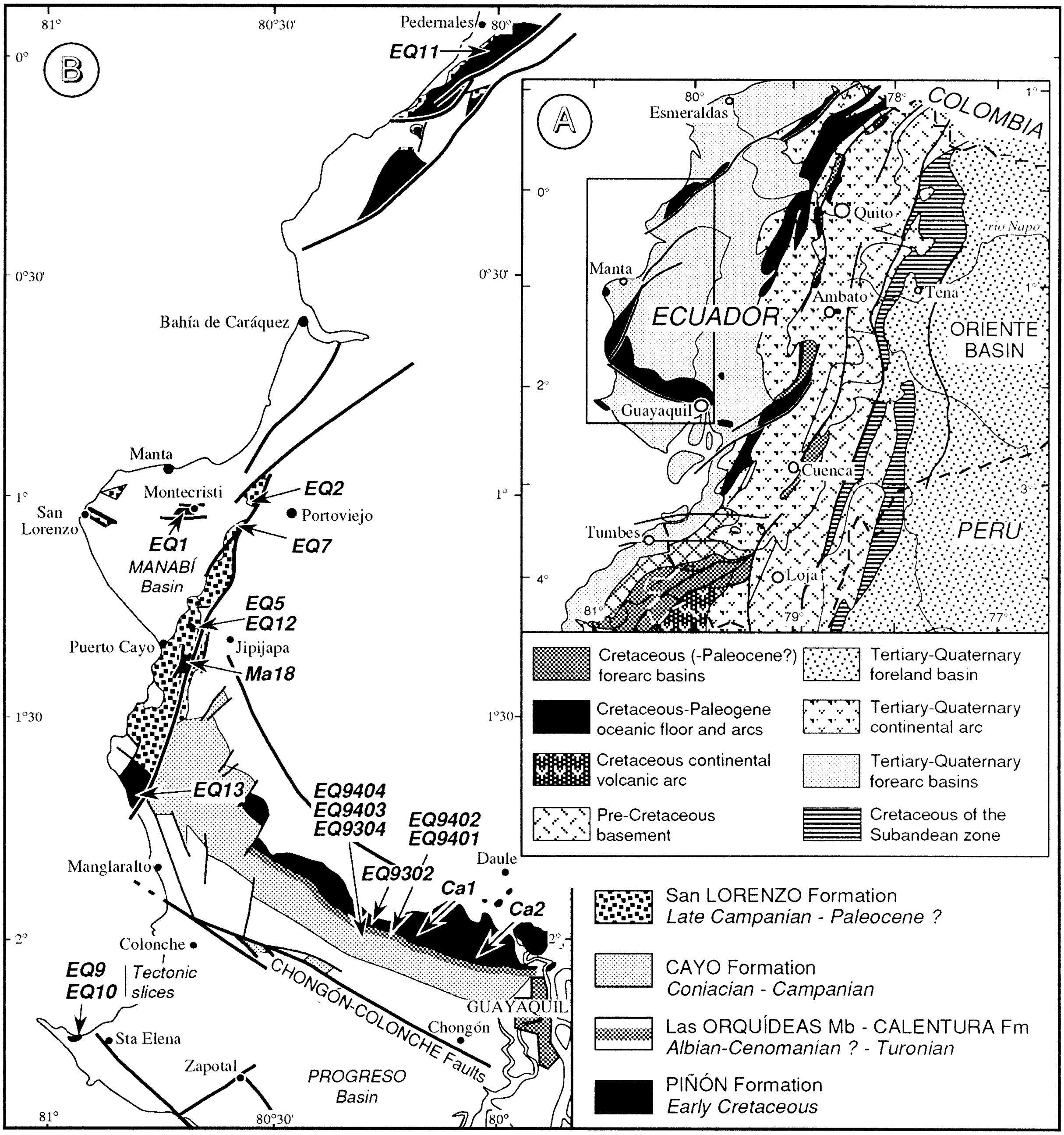

Fig. 1. (A) Schematic geological map of Ecuador showing the main geological and tectonic units and the location of the studied area. (B) Geological sketch of southern coastal Ecuador showing the distribution of the studied magmatic units and the location of the samples analyzed.

deformed area, where good and continuous sections can be observed, except locally, south of the Chongón–Colonche faults. In the Guayaquil outskirts (Las Orquídeas locality, Perimetral section) and in the Chogón–Colonche Cordillera, the undated Piñón Formation is overlain by a thin layer of pil-

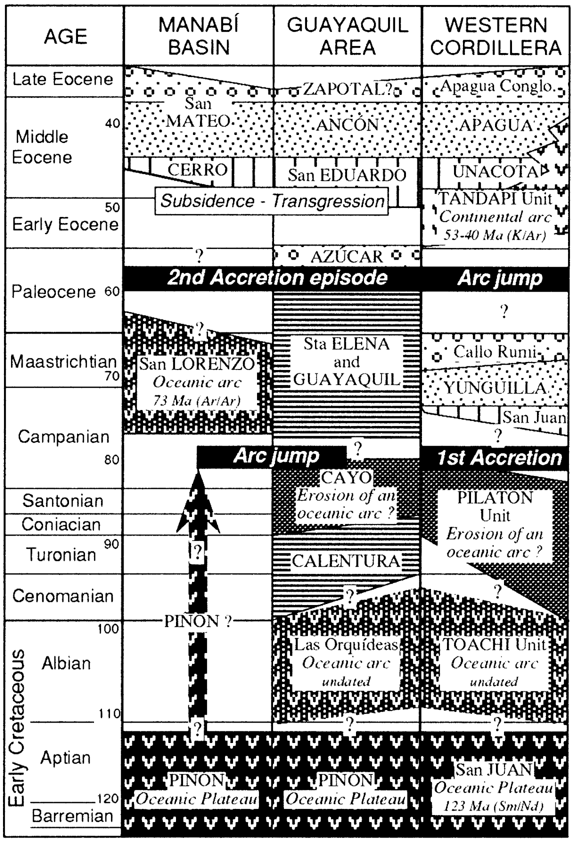

Fig. 2. Stratigraphic nomenclature and geodynamic setting of the Cretaceous–Tertiary rocks of western Ecuador.

lowed phyric basalts, referred to here as the Las Orquídeas Member (Fig. 2). Along the Perimetral section, the Las Orquídeas Member is stratigraphically overlain by a 200-m-thick succession of pelagic black shales, limestones and thin-bedded volcanic or volcaniclastic intercalations (Calentura Formation), which yielded Cenomanian to Turonian microfauna, a Turonian ammonite and Turonian to Coniacian nannofossils (Thalmann, 1946; Sigal, 1969; review in Jaillard et al., 1995). Therefore, the Las Orquídeas Member is of pre-Cenomanian to pre-Turonian age (~pre-95 Ma), and the underlying Piñón Formation is most probably of pre-Late Cretaceous age (Fig. 2).

The Calentura Formation is stratigraphically overlain by a 2000-m-thick turbiditic series of shales, greywackes and conglomerates (Cayo Formation). The Cayo Formation, of Coniacian to Campanian age, is interpreted as the product of the erosion of an island arc (Thalmann, 1946; Wallrabbe-Adams, 1990; Benítez, 1995). It is gradually overlain by about 400 m of pelagic dark shales, cherts, siliceous tuffs and subordinate thin-bedded turbidites (Guayaquil Formation, Fig. 2). The Guayaquil Formation, of Maastrichtian to early-Late Paleocene age (Thalmann, 1946; Faucher et al., 1971; Jaillard et al., 1995), is devoid of continental sediments.

South of the Chongón–Colonche fault, the Santa Elena Formation is a strongly deformed equivalent of the Guayaquil Formation (Sinclair and Berkey, 1924; Thalmann, 1946; Jaillard et al., 1995). The Santa Elena Formation is affected by gently dipping shear planes and tight folds exhibiting penetrative axial-plane cleavage, with evidence of northward thrusting. It is unconformably overlain by a 2000-m-thick series of quartz-rich megaturbidites of latest Paleocene to earliest Eocene age (Azúcar Fm., Jaillard et al., 1995). This major tectonic event of Late Paleocene age (~57 Ma) is interpreted as the result of the accretion of this area to the Andean margin (Jaillard et al., 1997).

In the whole coastal Ecuador, the Cretaceous–Paleocene volcanic and volcaniclastic rocks are unconformably overlain by a shallowing-upward sedimentary sequence of late-Early Eocene to Late Eocene age (Benítez, 1995; Jaillard et al., 1995; Fig. 2).

In this work, we shall use the same name (Piñón Formation) for the igneous basement of the Manabí and Guayaquil areas, although they are possibly not of the same age.

3. Analytical procedures and low-grade metamorphism of the igneous rocks of western Ecuador

Samples have been collected from the igneous basement (Piñón Formation), the Las Orquídeas Member and the San Lorenzo and Cayo Formations (Fig. 1). Fourteen samples were analyzed for major, minor and trace elements (Table 2). Among these samples, Nd–Sr isotopic compositions were determined on nine of the less altered ones (Table 3). The location of these samples (Fig. 1) and their petrographic characteristics are listed in Table 1.

3.1. Analytical procedures

Major and minor elements were analyzed by G. Mevelle at the Centre de Recherche Pétrographiques et Géochimiques (CRPG) of Nancy. Trace elements, including the REE, were analyzed by ICP–MS using acid dissolution of 100 mg sample at the Laboratoire de Géochimie isotopique de l'Université Paul Sabatier in Toulouse following the procedure of M. Valladon et al. (unpubl. report). 100 mg of powdered rocks are weighed in a Pt crucible, with 320 mg Lithium metaborate and 80 mg Lithium borate (Fluka). After careful mixing of the powders, the crucible is heated for fusion at 1000ºC. After cooling, 8 ml double-distilled HNO_3 (12 N) and HF are added for the dissolution of the glass. The final dilution to 30 ml of a 15-ml aliquot, with MilliQ™ water and after addition of internal standards (In-Re), corresponds to a total dilution of 3000. Limits of detection are: REE and Y = 0.03 ppm, U, Pb and Th = 0.5 ppm, Hf and Nb = 0.1 ppm, Ta = 0.03 ppm, and Zr = 0.04 ppm. Standards used for the analyses were JB2, WSE Bir-1 and JR1. Analysis of sample EQ12 was duplicated following the procedure of Barrat et al. (1996).

For Sr and Nd isotopic analyses, samples were leached twice in a 2 N HCl–0.1 HF mixture. For Pb isotope determinations, whole rocks were successively leached in hot 2 N HCl for 20 min in an ultrasonic bath, rinsed with tri-distilled water, leached in cold 1 N HNO_3 for 20 min and rinsed with tri-distilled water in an ultrasonic bath during 15 min.

Nd and Sr isotopic compositions were determined on a Finnigan MAT 261 multicollector mass spectrometer at the Laboratoire de Géochimie isotopique de l'Université Paul Sabatier in Toulouse, using the analytical procedures of Lapierre et al. (1997). Correction of the mass discrimination effect was done by normalizing the $^{88}Sr/^{86}Sr$ ratio to a value of 8.3752. NBS 987 standard was measured with a $^{87}Sr/^{86}Sr$ ratio of 0.71025 ($\pm$22). Measured $^{143}Nd/^{144}Nd$ were normalized to a value of $^{146}Nd/^{144}Nd = 0.71219$ (Wasserburg et al., 1981). Results on La Jolla standard yielded $^{143}Nd/^{144}Nd = 0.511850 \pm 8$ (mean on 39 runs) corresponding to an external reproducibility of 0.00001.

$^{206}Pb/^{204}Pb$, $^{207}Pb/^{204}Pb$ and $^{208}Pb/^{204}Pb$ isotopic ratios were measured on a multicollector VG sector mass spectrometer at the Laboratoire de Géochimie isotopique de l'Université de Montpellier II (Table 3) following the analytical procedure adapted from Manhès et al. (1980). Total Pb blanks are less than 65 pg for a 100 mg sample.

3.2. Metamorphism and alteration of the igneous rocks of western Ecuador

All the igneous rocks of western Ecuador, with the exception of the arc-rocks of San Lorenzo Formation, are metamorphosed to a low-grade zeolite and prehnite–pumpellyite facies, and igneous textures are always preserved. In the analyzed samples, clinopyroxene remains fresh while orthopyroxene is replaced by smectites $\pm$ chlorites. When altered, clinopyroxene is replaced by smectites, chlorites or colourless actinolite. Plagioclase is often replaced by sericite or calcite but sometimes remains fresh. However, in the arc-lavas of the Las Orquídeas Member, plagioclase is albitized. Vesicules are filled by smectite, chlorite, epidote and pumpellyite, which are also present in the groundmass which sometimes includes abundant chalcedony (EQ94-02; Table 1). Glass is systematically recrystallized in brown reddish or pale to intense green smectites.

Hydrothermal alteration of hypabyssal volcanic rocks may cause significant mobility of some major (Na, K, Ca, Si) and trace elements (Rb, Ba, Sr), while Na_2O contents (2–4 wt%; Table 2) are relatively homogeneous. K_2O ($\leq$1.3 wt%; Table 2) and Rb ($0.3 <$ Rb ppm < 11.8; Table 2) are more scattered and most likely express rock alteration. The weight loss on ignition (LOI) ranges between 2.1 and 7.6% (Table 2). LOI generally positively correlates with CaO abundance due to the presence of epidote and minor calcite.

In this study, alkali (K, Rb, and Na) and alkaline earth (Sr, Ba, Ca) elements and SiO_2 are only presented as background information and only the less mobile elements Ti, Nb, Th, Ta, Zr, Hf and REE are used for the geochemical discussion.

4. Basement of southern coastal Ecuador (Piñón Formation)

4.1. Petrology and mineral chemistry

The igneous components of the Piñón Formation consist of olivine-free basalts and dolerites (Table 1).

Table 1
Location and petrographic characteristics of the Cretaceous–Paleocene igneous rocks from western Ecuador

Formation:	Piñón	Piñón	Piñón	Piñón	Piñón	Piñón
Sample:	EQ93.02	EQ1	EQ5	EQ10	Ca1	Ca2
Location:	Las Piedras	Montecristi	Puerto Cayo	La Libertad	Sabaneta	Petrillo
Texture:	Intersertal + quenched vesicular	Aphyric + quenched	Intersertal	Ophitic	Intersertal	Intersertal
Mineralogy:	Plagioclase laths and microlites + augite Fe–Ti oxides	Plagioclase associated or not with augite clots	Zoned plagioclase laths, subeuhedral augite	Plagioclase laths	Plagioclase laths and microlites + augite Fe–Ti oxides	Plagioclase laths and microlites + augite minor Fe–Ti oxides
	Glass replaced by smectites	titanomagnetite	titanomagnetite	anhedral augite	Glass replaced by smectites	
		Abundant glass replaced by smectites	Glassy pods replaced by smectites	anhedral titanomagnetite		
Name:	Basalt	Basalt	Diabase	Diabase	Basalt	Basalt

Formation:	Piñón	Piñón	Piñón	Las Orquídeas	Las Orquídeas	San Lorenzo	San Lorenzo
Sample:	EQ11	EQ12	EQ13	EQ94.01	EQ94.02	EQ2	EQ7
Location:	Pedernales	Puerto Cayo	Riconada	Las Orquídeas	Cerro Jordan	Cerro de Hoja	La Pila
Texture:	Intersertal	Intersertal	Porphyritic + quenched	Porphyritic + quenched	Porphyritic + intersertal	Ophitic and porphyritic	Porhyritic + fluidal
Mineralogy:	Plagioclase laths and microlites + clinopyroxene Fe–Ti oxides	Plagioclase laths	Plagioclase + clinopyroxene phenocrysts + microlites	Plagioclase + Opx + Cpx pseudomorphs	Mg-rich augite phenocrysts + Fe–Ti oxides	Euhedral labrador + augite with Ti-rich magnetite inclusions	Labrador + zoned Ca-rich cpx phenocrysts
	Glass replaced by smectites	Clinopyroxene	abundant glassy groundmass with few Fe–Ti oxides	groundmass recrystallized in smectites + chlorites	Groundmass rich in plagioclase laths and microlites		groundmass with plagioclase microlites
		abundant large titanomagnetite crystals					
Name:	Basalt	Ferro-diabase	Basalt	Tholeiitic Basalt	Calc-alkaline Basalt	Calc-alkaline Diabase	Calc-alkaline Andesite

Table 2
Major- and trace-element concentrations of igneous oceanic rocks from western Ecuador

	Oceanic plateau–Piñón Formation											Intra-oceanic arc			
Sample No.:	EQ93.02 [a]	EQ1 [a]	EQ5 [a]	EQ10	Ca1 [a]	Ca2	EQ11 [a]	EQ12	EQ12	EQ13	MA18	EQ94.01 [a]	EQ94.02 [a]	EQ2	EQ7 [a]
Name:	Basalt	Basalt	Dolerite	Dolerite	Basalt	Basalt	Basalt	Dolerite	Duplicate	Basalt	Dolerite	Basalt	Basalt	Diabase	Basalt
SiO_2 (wt%)	52.01	48.88	48.45	48.83	50.87	51.56	50.4	54.2		48.95		57.82	63.4	52.29	52.2
TiO_2	1.06	1.23	1.61	1.58	1.55	1.08	1.36	2.1		1.16		0.24	0.23	0.91	0.95
Al_2O_3	14.89	14.39	16.1	15.2	13.2	13.75	13.93	13.34		14.86		14.83	12.93	16.22	16.32
Fe_2O_3 [b]	12.17	12.75	14.05	12.32	14.73	12.87	14.1	16.64		12.05		9.46	8.43	11.9	12.18
MnO	0.16	0.2	0.2	0.24	0.19	0.18	0.22	0.23		0.2		0.09	0.12	0.17	0.19
MgO	7.58	8.96	6.57	6.4	6.69	7.36	7.24	3.1		8.38		8.65	5.11	5.1	4.48
CaO	7.7	10.81	9.94	11.4	8.3	9.86	9.02	5.79		11.54		4.57	7.23	8.8	9.4
Na_2O	4.3	1.89	2.34	2.95	3.91	3.68	3.1	4.09		2.5		4.29	2.31	2.88	2.92
K_2O	0.00	0.72	0.55	0.9	0.18	0.15	0.27	0.13		0.16		0.00	0.09	1.38	0.99
P_2O_5	0.13	0.18	0.19	0.17	0.18	0.14	0.18	0.29		0.16		0.05	0.13	0.34	0.39
LOI	2.99	4.45	3.18	4.32	2.72	2.15	5.94	2.81		5.64		7.63	2.24	2.16	3.75
Cr (ppm)	236.00	284.84	8.73	54.01	–	–	–	–		–		785.00	210.00	49.59	36.54
V	327.00	353.12	433.49	422.62	509.92	413.46	459.77	64.11		398.13		119.00	144.00	421.12	418.98
Sc		61.49	53.91	51.69	81.49	75.97	79.86	40.34		78.72				33.22	38.95
Ni	98.1	100.73	32.72	52.49	82.95	84.76	67.76	4.58		121.05		177.00	46.5	25.41	20.16
Rb	0.3	5.24	3.5	11.81	6.01	4.02	4.66	1.61	1.26	6.44		0.09	1.06	24.35	17.54
Rb	0.3	5.24	3.5	11.81	6.01	4.02	4.66	1.61		6.44	1.22	0.09	1.06	24.35	17.54
Sr	66.00	110.69	130.8	117.67	160.82	121.42	201.58	116.12	110.00	208.21	110.00	114.00	242.00	441.55	545.6
Y	19.6	22.26	23.16	20.45	38.38	25.92	33.58	51.02	57.01	22.69	16.9	4.5	5.8	20.45	23.5
Zr	44.00	60.09	24.75	30.68	86.39	40.81	73.32	77.07	165.00	62.67	34.00	22.00	45.00	87.97	105.94
Nb	3.13	4.16	4.29	4.18	5.34	3.87	4.66	10.75	11.71	3.92	2.69	0.63	1.28	1.22	1.42
Cs	0.01	0.00	0.00	0.18	0.11	0.05	0.03	0.01	28.21	0.13		0.01	0.16	0.46	0.56
Ba	29.00	14.9	36.35	35.5	392.35	–	–	–	23.38	–	21.00	13.00	108.00	263.95	266.7
La	2.68	3.5	4.09	3.37	5.29	3.68	4.3	9.25	9.49	3.2	2.27	1.42	2.69	10.57	13.13
Ce	7.02	9.63	10.68	9.18	14.17	9.66	11.35	24.49	25.16	8.9	6.28	2.75	6.08	24.7	30.88
Pr	1.07	1.56	1.71	1.51	2.25	1.52	1.8	3.8	3.80	1.43	1.08	0.44	0.83	3.92	4.83
Nd	5.63	8.11	8.59	7.87	11.89	8.15	9.5	19.53	18.69	7.66	5.48	2.11	3.83	17.96	22.42
Sm	1.85	2.57	2.66	2.42	3.91	2.67	3.12	6.11	5.95	2.51	1.91	0.59	1.00	4.17	5.08
Eu	0.71	0.96	1.06	0.95	1.37	1.03	1.17	2.19	2.06	0.96	0.78	0.25	0.36	1.24	1.44
Gd	2.73	3.46	3.58	3.25	5.6	3.89	4.68	8.37	7.54	3.65	2.38	0.76	1.16	4.02	4.82
Tb	0.49	0.66	0.68	0.59	1.05	0.71	0.85	1.47	1.39	0.67	0.47	0.12	0.17	0.65	0.75
Dy	3.4	4.4	4.5	4.04	7.09	4.81	5.89	9.56	9.21	4.56	3.06	0.77	1.00	3.99	4.59
Ho	0.74	0.9	0.93	0.81	1.57	1.04	1.3	1.96	2.00	0.99	0.67	0.16	0.2	0.8	0.9
Er	2.06	2.6	2.57	2.24	4.59	3.05	3.82	5.48	5.77	2.85	1.82	0.44	0.55	2.28	2.6
Tm	0.309	0.39	0.35	0.32	0.66	0.43	0.58	0.77	nd	0.42	0.28	0.066	0.083	0.33	0.37
Yb	2.05	2.53	2.27	2.01	4.62	2.99	3.9	5.17	5.57	2.78	1.74	0.44	0.54	2.18	2.41
Lu	0.319	0.38	0.35	0.31	0.72	0.47	0.61	0.77	0.87	0.41	0.27	0.075	0.093	0.35	0.37
Hf	1.33	1.89	0.96	1.09	2.76	1.54	2.24	2.49	4.63	2.07	1.18	0.59	1.17	2.53	3.07
Ta	0.242	0.58	0.25	0.32	0.4	0.28	0.33	0.67	0.74	0.3	0.18	0.033	0.092	0.03	–
Pb	0.56	0.14	0.00	0.00	0.505	0.305	0.315	0.222	0.29	0.391	2.89	0.52	1.87	2.95	3.96
Th	0.26	0.25	0.11	0.13	0.53	0.35	0.43	0.43	0.63	0.29	0.18	0.15	0.43	1.16	1.44
U	0.07	0.08	0.02	0.1	0.14	0.08	0.11	0.1	0.22	0.09	0.06	0.06	0.79	0.49	0.63
Eu/Eu [b]	0.97	0.98	1.04	1.05	0.89	0.97	0.93	0.93		0.96	1.11	1.14	1.02	0.93	0.89
$(La/Yb)_N$	0.94	0.99	1.29	1.2	0.82	0.88	0.79	1.28		0.83	0.88	2.31	3.57	3.48	3.91

[a] Analyzed for isotopic composition. Major elements reported on volatile-free basis.
[b] Total iron reported as Fe_2O_3.

The basalts show intersertal (EQ93-02, Ca1, EQ11) to aphyric (EQ1) textures. The intersertal basalts consist of plagioclase laths and clinopyroxene glomeroporphyric aggregates embedded in a glass-poor groundmass which contains small rounded vesicules filled with smectites + epidote ± chalcedony and quenched plumose or dendritic clinopyroxene crystals. The size of the plagioclase laths is highly variable and ranges from 0.1 to 1 mm. Fresh plagioclase shows a labradorite composition (An_{66}). Fe–Ti oxides are sometimes TiO_2-rich (24.5%). The aphyric basalts are formed of clinopyroxene aggregates either or not associated with plagioclase set in a glass-rich groundmass which includes isolated plagioclase microphenocrysts. In both lavas, Fe–Ti oxides are anhedral and the last mineral to precipitate.

The dolerites exhibit ophitic (EQ9, EQ10) to intersertal textures (EQ5) and are composed of plagioclase laths enclosed in anhedral clinopyroxene. Euhedral plagioclase is zoned with labradorite cores (An_{69}) and oligoclase rims (An_{12}). The dolerites differ with the size of the clinopyroxene and Fe–Ti oxides and the abundance of interstitial glass. Subhedral clinopyroxene and anhedral Fe–Ti oxides may occur as large crystals up to 1 cm and 0.5 cm, respectively. Oxides are titanomagnetites ($TiO_2 \leq 10\%$) with ulvospinel ($21 < TiO_2\% < 52$) fine exsolution lamellae. Orthopyroxene may occur.

The weakly zoned clinopyroxene shows similar composition in the basalts and dolerites; it is an augite ($Wo_{39–43}$, $En_{41–47}$ $Fs_{9–15}$; Morimoto, 1988) with slightly Fe-enriched rims.

4.2. Geochemistry

The basalts and dolerites have restricted SiO_2, Al_2O_3, and TiO_2 ranges (Table 2). Basalts and dolerites have similar MgO contents (Table 2; Fig. 3) with the exception of a dolerite (EQ12) which has a lower MgO content and correlatively higher Fe_2O_3, TiO_2, Nb and Y abundances (Fig. 3). This rock represents the most fractionated rock of the suite (Table 2). At similar MgO levels, basalts and dolerites (except EQ12) have a large range of Zr and Y concentrations while their Nb contents range only between 3 and 5 ppm (Table 2; Fig. 3). TiO_2 increases while MgO decreases (Fig. 3). Both rocks show high Ti/V ($19.5 < Ti/V < 23$) and low La/Nb (<1) ratios.

Basalts and dolerites show flat REE patterns ($0.8 < (La/Yb)_{CN} < 1.3$; Fig. 4) relative to chondrite (Sun and McDonough, 1989). However, two groups may be distinguished on the basis of the $(La/Yb)_N$ ratios. Group 1, composed of the basalts, is characterized by slightly depleted LREE patterns with $(La/Yb)_{CN} < 1$ (Fig. 4A), whereas Group 2 dolerites exhibit slightly LREE-enriched patterns with

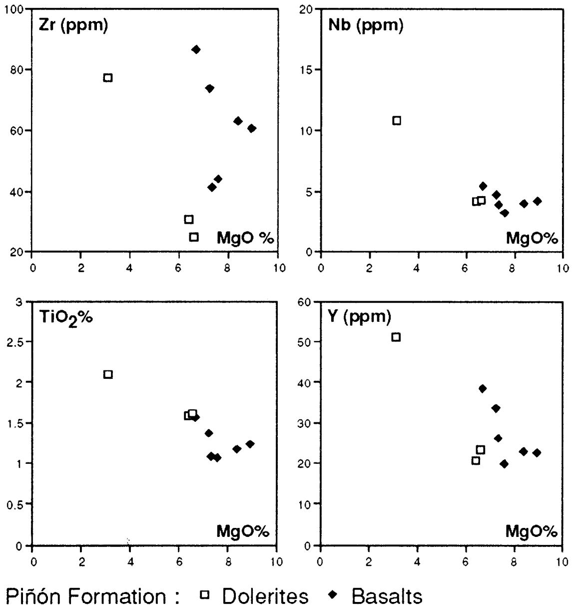

Fig. 3. Zr (ppm), Nb (ppm), TiO_2 (wt%) and Y (ppm) vs. MgO (wt%) correlation diagrams of the basalts and dolerites of the Piñón Formation.

$(La/Yb)_{CN}$ ratios >1 (Fig. 4B). In both groups, small negative or positive Eu anomalies (Table 2) may reflect minor plagioclase removal or accumulation, respectively.

Relative to N-type MORB (Sun and McDonough, 1989; Fig. 5), these basalts and dolerites show significant enrichments in LREE, high Nb, Ta and Th values (1.5–5 times the N-MORB values), and low levels in Zr and Hf (0.3–1 times the N-MORB values. The distinction into two groups for the igneous rocks of the Piñón Formation is also valid with respect to their N-MORB-normalized trace element patterns. Group 1 is Th-, Ta- and Nb-enriched and shows a mild depletion in Zr and Hf (Fig. 5A). Group 2 dolerites differs from Group 1 by the lack of Th enrichment (specially marked in the EQ10 and EQ12 samples) and more marked Zr and Hf negative anomalies (Fig. 5B). In both Group 1 and 2, the HREE and Y contents are more or less similar to those of N-MORB or slightly higher (3 times the N-MORB values for the most fractionated rocks). Moreover, Nb/Ta and Zr/Hf ratios of these rocks are lower than those of N-MORB but U/Th is higher (Fig. 6). The basalts and one dolerite have a rather restricted range of Nb/U ratios (38 <

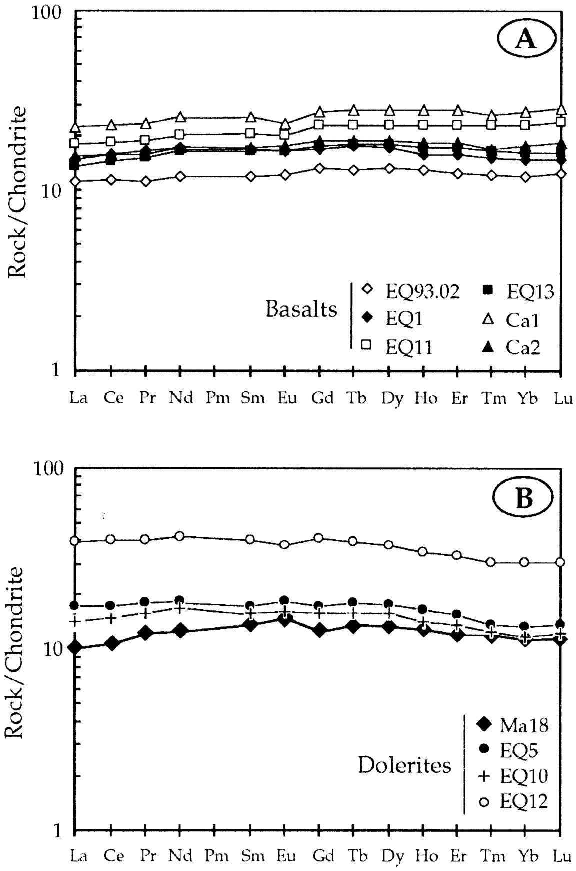

Fig. 4. Chondrite-normalized (Sun and McDonough, 1989) rare earth elements patterns of the basalts (A) and dolerites (B) of the Piñón Formation.

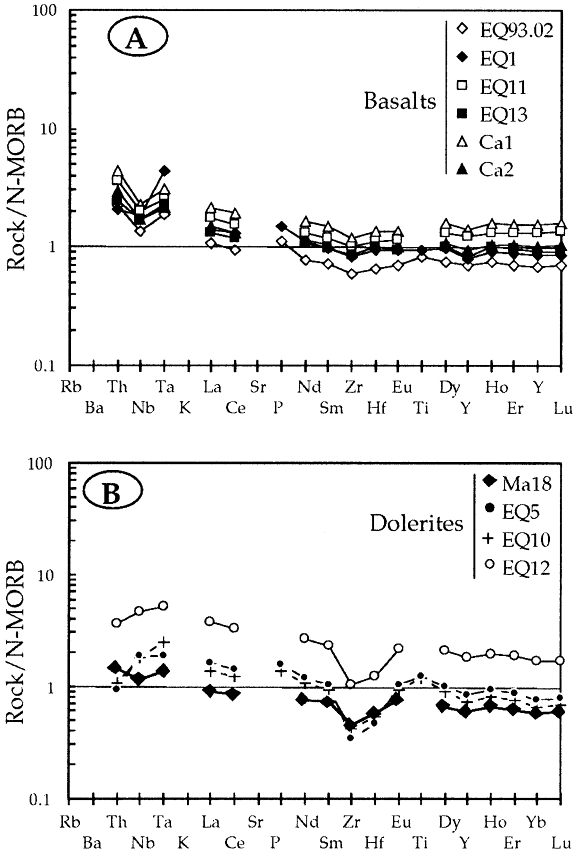

Fig. 5. N-MORB-normalized (Sun and McDonough, 1989) spidergrams of the basalts (A) and dolerites (B) of the Piñón Formation.

Nb/U $<$ 52; Fig. 6) which are slightly higher than those of N-MORB (Fig. 6), but fall within the range of oceanic mantle (Nb/U $= 47 \pm 10$; Hofmann, 1988). Two dolerites (EQ5 and EQ2) differ from the basalts by significantly higher Nb/U ratios (107 and 214; Table 2), which reflects, most likely, postmagmatic addition of U.

Thus, the basalts and dolerites of the Piñón Formation show oceanic plateau basalt affinities but differ on some trace element distribution (i.e. LREE, Zr, Hf and Th).

4.3. Nd and Sr and Pb isotopic composition

Isotopic data on the basalts and dolerites of the Piñón Formation have been corrected for in-situ decay with an age of 123 Ma (see below the discussion on the age of the Piñón Formation).

Basalts and dolerites display variable ε_{Nd} ratios which range between +4.5 (Ca1) and +10 (EQ1, Table 3; Fig. 7). Two dolerites (EQ5, MA18) and two basalts (EQ93-02, EQ11) show homogeneous ε_{Nd} ratios of +7. With the exception of EQ1, being similar to N-MORB, these ε_{Nd} ratios fall within the range of ocean island basalts (OIB).

All the Piñón igneous rocks display a large range of $(^{87}Sr/^{86}Sr)_i$ ratios (0.70435 to 0.70466), except for two samples (EQ1 and EQ5) which have lower $(^{87}Sr/^{86}Sr)_i$ ratios (0.70321 and 0.70335, respectively; Table 3; Fig. 7).

At similar Zr/Nb (~15) and $(La/Yb)_{CN}$ (~0.8–0.9) ratios the basalts and one dolerite (MA18) dis-

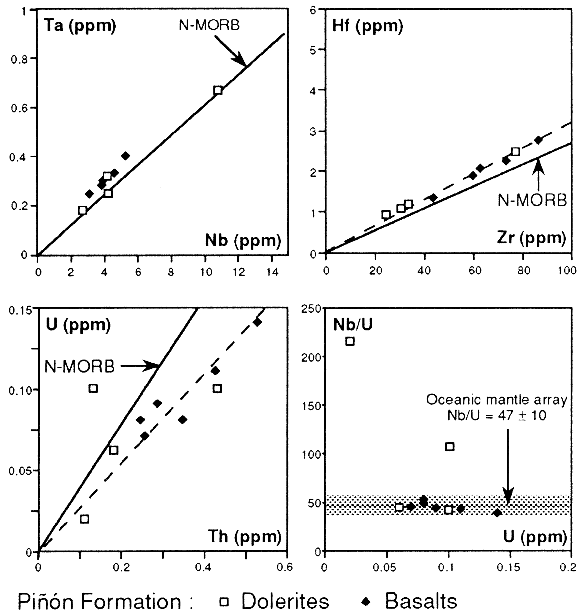

Fig. 6. Ta–Nb, Hf–Zr, U–Th, Nb/U–U correlations diagrams of the basalts and dolerites of the Piñón Formation. Altered samples have been omitted in the U–Th and Nb/U–U diagrams.

play a large range of ε_{Nd} ratios (+10 to +4), except for dolerite EQ5 having lower Zr/Nb (5.8) and higher $(La/Yb)_{CN}$ (1.3; Fig. 7).

Initial lead isotopic compositions of whole rock and mineral separates display a large range in composition (Table 3; Fig. 8; Lapierre et al., 1999). EQ12 has the lowest $^{206}Pb/^{204}Pb$ ratio and plots near DMM source while Ca1 has the higher $^{206}Pb/^{204}Pb$ ratio similar to those of recent Galápagos lavas. The high $^{207}Pb/^{204}Pb$ ratios of these rocks could indicate minor amounts of pelagic sediments (Doe, 1970) in the mantle source.

EQ1 has the highest ε_{Nd} ratio (+10), reflecting derivation from the most depleted component. However, the $(^{206}Pb/^{204}Pb)_i$ of this rock is higher (18.16) than that of the Piñón lavas, due to the high content of U relative to Th. Indeed, this rock does not plot on the Th/U correlation trend but is displaced towards the U side of the diagram (Fig. 6). This reflects the mobility of U linked to a hydrothermal event which affected EQ1. In contrast, Ca1 is characterized by the lowest ε_{Nd} (+4) and the highest $^{206}Pb/^{204}Pb$ (18.92) ratios, suggesting derivation from a more enriched source.

Table 3
$^{87}Sr/^{86}Sr$ and $^{143}Nd/^{144}Nd$ isotope ratios of igneous oceanic rocks from western Ecuador

Formations	Samples	t (Ma)	$^{87}Rb/^{86}Sr$	$^{87}Sr/^{86}Sr$	$(^{87}Sr/^{86}Sr)_i$	ε_{Sr}	$^{147}Sm/^{144}Nd$	$^{143}Nd/^{144}Nd$	$(^{143}Nd/^{144}Nd)_i$	ε_{Nd}	$(^{206}Pb/^{204}Pb)_i$	$(^{207}Pb/^{204}Pb)_i$	$(^{207}Pb/^{204}Pb)_i$
Piñón Fm.	EQ93.02	123	0.01314	0.704686 ± 10	0.7046	**+4.37**	0.1986	0.513 ± 11	0.512840	**+7.03**			
	EQ1	123	0.1369	0.703451 ± 27	0.7032	**−16.24**	0.1916	0.513154 ± 25	0.512999	**+10.14**	18.159	15.529	37.840
	EQ5	123	0.07738	0.703487 ± 21	0.7033	**−14.25**	0.1872	0.513004 ± 14	0.512853	**+7.29**			
	EQ11	123	0.06686	0.704936 ± 25	0.7048	**+6.58**	0.1985	0.513028 ± 8	0.512868	**+7.58**			
	Ca1	123	0.10809	0.704542 ± 17	0.7043	**−0.03**	0.1988	0.51287 ± 7	0.512710	**+4.49**	18.923	15.566	38.431
	MA18	123					0.2107	0.513047 ± 6	0.512877	**+7.76**			
	EQ12	123	0.0401	0.703561 ± 12	0.70349	**−12.27**	0.1891	0.703561 ± 12	0.51287	**+7.69**	17.414	15.548	37.166
	PiO4	123	0.0148	0.703506 ± 11	0.70348	**−12.43**	0.2119	0.513008 ± 6	0.51284	**+6.98**	17.898	15.595	37.825
Las Orquídeas Mb.	EQ94.01	100	0.00228	0.70467 ± 10	0.7046	**+4.04**	0.169	0.512986 ± 11	0.512875	**+7.14**			
	EQ94.02	100	0.01266	0.704095 ± 10	0.7040	**−4.34**	0.1578	0.512921 ± 11	0.512817	**+6.02**			
San Lorenzo Fm.	EQ7	75	0.09297	0.703541 ± 19	0.7034	**−13.77**	0.1369	0.512961 ± 16	0.512893	**+6.87**			

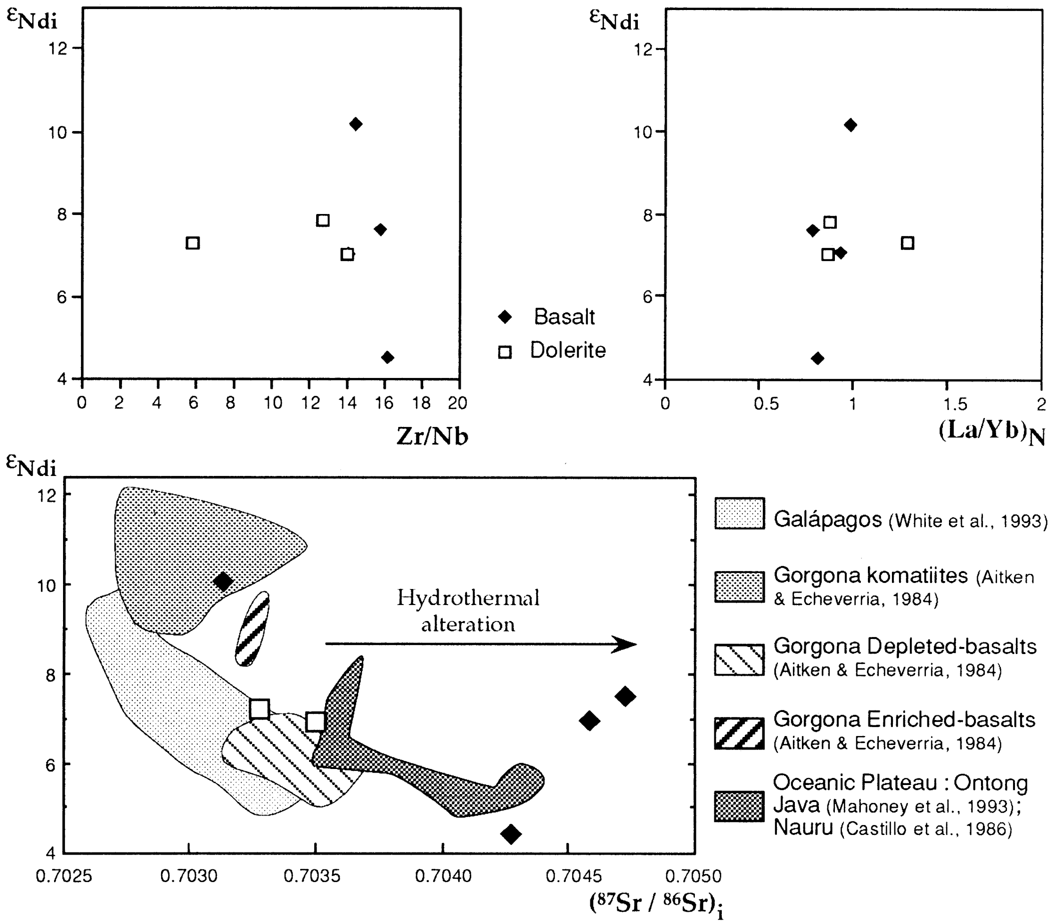

Fig. 7. $\varepsilon_{Nd,i}$–Zr/Nb (A), $\varepsilon_{Nd,i}$–$(La/Yb)_N$ (B) and $\varepsilon_{Nd,i}$–$(^{87}Sr/^{86}Sr)_i$ (C) correlation diagrams for the basalts and dolerites of the Piñón Formation (data from Aitken and Echeverria (1984) and Castillo et al. (1986), among others).

4.4. Summary and comparisons

The basalts and dolerites of the Piñón Formation show flat REE patterns and Ta- and Nb-enrichments relative to N-MORB (Fig. 9). The basalts are slightly depleted in LREE, TiO_2, Ta, and Nb relative to dolerites and some basalts show higher Th contents than the dolerites. The Piñón basalts and dolerites display a rather restricted range of ε_{Nd} (+7.03 to +7.76) and $(^{206}Pb/^{204}Pb)_i$ ratios (17.41 to 17.90), with the exception of two rocks. As a whole, they are interpreted as the products of an oceanic plateau.

Basalts and dolerites of the Piñón Formation are probably older than the Late Cretaceous (92–88 Ma) Caribbean–Colombian Oceanic Plateau Province (CCOP) basalts. In coastal Ecuador, the Piñón basalts are stratigraphically overlain by Cenomanian to Coniacian (99–87 Ma; Haq and Van Eysinga, 1998) pelagic sediments. Basalts and dolerites of the Piñón Formation are less radiogenic in Pb than the CCOP basalts and the Galápagos recent lavas (Fig. 8; Lapierre et al., 1999). This suggests that the oceanic plateau tholeiites of the Piñón Formation derived from mantle(s) source(s) depleted in isotopic Pb, compared to those of the Galápagos hotspot. So, the plume that generated the Piñón Formation oceanic plateau is likely different from, and probably older than the hotspot responsible for the formation of the CCOP and/or the Galápagos.

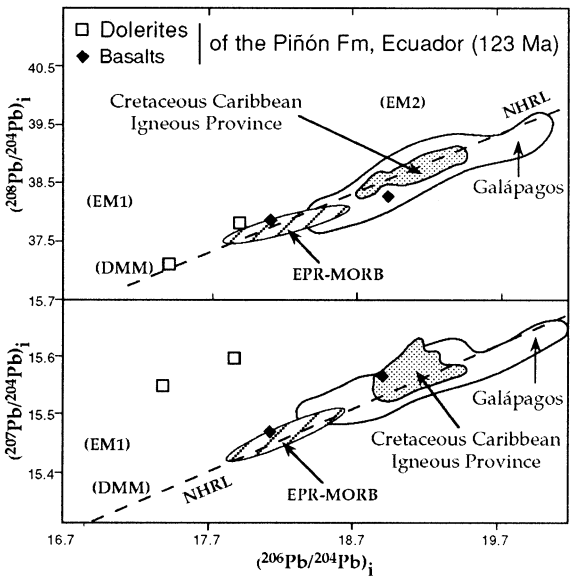

Fig. 8. $(^{208}Pb/^{204}Pb)_i$ vs. $(^{206}Pb/^{204}Pb)_i$ and $(^{07}Pb/^{204}Pb)_i$ vs. $(^{206}Pb/^{204}Pb)_i$ correlation diagrams for the basalts and dolerites of the Piñón Formation. Data from the Nicoya and Herradura (90 Ma) igneous complexes (Costa Rica) after Hauff et al. (1997) and Sinton et al. (1997, 1998). Fields of the Gorgona picrites, komatiites, tholeiites and K-tholeiite are after Dupré and Echeverria (1984). The field of the Dumisseau basalts from Haiti is from Sen et al. (1988). East Pacific MORB and Galápagos Island are from White et al. (1987, 1993). *NHRL* = North Hemisphere Line after Hart (1984).

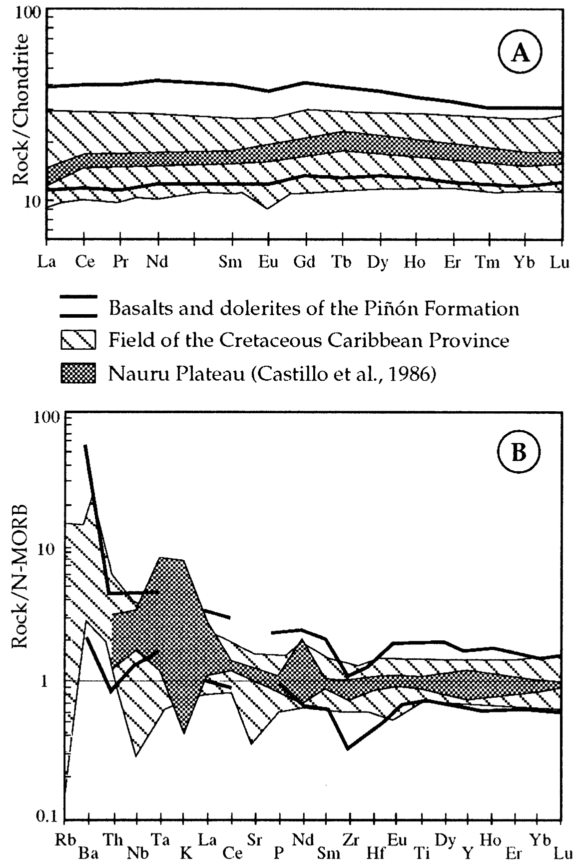

Fig. 9. Trace-element geochemical similarities of the basalts and dolerites of the Piñón Formation with Late Cretaceous oceanic plateau basalts from Hispaniola and western Colombia and ocean floor basalts of the Nauru Plateau.

5. Upper Cretaceous(–Lower Paleocene?) lavas (Las Orquídeas Member, Cayo and San Lorenzo Formations)

5.1. Petrology and mineral chemistry of the lavas and volcaniclastic sediments

The igneous rocks of the Upper Cretaceous–Lower Paleocene island arcs are mafic lavas and dolerites sampled in the Las Orquídeas Member and San Lorenzo Formation (Figs. 1 and 2; Tables 1 and 2). In southern coastal Ecuador, the Cayo Formation consists solely of volcaniclastic sediments.

The basalts from the Las Orquídeas Member are plagioclase–pyroxene phyric (Table 1). EQ94-01 consists of plagioclase, orthopyroxene and clinopyroxene pseudomorphs set in a glass-rich groundmass which includes small amounts of clinopyroxene and plagioclase and very few oxides. EQ94-02 exhibits an intersertal texture with preserved clinopyroxene phenocrysts of augitic composition ($Wo_{37–42}$, $En_{49–52}$, $Fs_{8–10}$) (Benítez, 1995). Fe–Ti oxides are included in the plagioclase and augite phenocrysts and thus represent early crystallizing crystals.

The igneous rocks of the San Lorenzo Formation are fresh compared to those of the Las Orquídeas Member. EQ2 is a dolerite (Table 1) which is formed of euhedral plagioclase and anhedral augite ($En_{42–44}$, $Fs_{20–17}$, $Wo_{38–39}$). Both plagioclase and clinopyroxene include TiO_2-rich magnetite (15 to 18%). Plagioclase occurs as large phenocrysts up to 1 cm long and small laths and exhibits a labradorite composition ($An_{52–63}$) with Na-rich rims. EQ7 is a porphyritic basaltic andesite (Table 1) which is formed of labradorite (An_{61-67}) and zoned clinopyroxene phenocrysts. Plagioclase includes euhedral Ti-rich magnetite crystals and shows locally bytownite (An_{75}) cores. Clinopyroxene shows diopsidic cores (En_{48}, Fs_6, Wo_{46}; Morimoto, 1988) rimmed by augite (En_{44}, Fs_{16}, Wo_{40}).

The studied samples of the Cayo Formation are volcanic breccias and greywackes. The volcanic breccias (EQ93.03, EQ94.04; Fig. 1) are composed of basaltic and andesitic fragments and pyroxene phenocrysts. When preserved, the pyroxenes show clinoenstatitic (En_{64-75}, Fs_{22-32}, Wo_{2-4}) and augitic (En_{43-44}, Fs_{16-19}, Wo_{38-41}) compositions (Benítez, 1995) which fall in the orogenic basalt field of Leterrier et al. (1982) diagrams (not presented here). The basaltic fragments are orthopyroxene–clinopyroxene–plagioclase–phyric. The andesite differs from the basalts by the abundance of plagioclase phenocrysts. The greywackes (EQ94.03; Fig. 1) consist of basaltic fragments, and phenocrysts of augite (En_{35-44}, Fs_{15-26}, Wo_{40-45}) and plagioclase, broken or not (Benítez, 1995).

5.2. Geochemistry

The igneous rocks of the Las Orquídeas Member and San Lorenzo Formation display calc-alkaline affinities (Fig. 10; Table 2) with the exception of EQ94.01 which exhibits an arc-tholeiitic affinity (Fig. 10; Table 2). These arc-rocks are LREE-enriched ($2.31 < (La/Yb)_{CN} = 3.57$; Fig. 10A) and their N-MORB-normalized element diagrams (Sun and McDonough, 1989; Fig. 10B) are very similar to those of orogenic suites. Moreover, the Las Orquídeas and San Lorenzo lavas possess a negative Nb–Ta anomaly, similar to arc-related volcanic rocks.

The lavas of the Las Orquídeas Member differ from rocks of the San Lorenzo Formation in that they have very low levels of Y and HREE (less than 10 times the chondritic values; Table 2; Fig. 10B), suggesting the presence of residual garnet in the mantle source.

5.3. Isotopic chemistry

The ages of 100 and 75 Ma have been taken to calculate the initial $^{87}Sr/^{86}Sr$ and ε_{Nd} ratios of the igneous rocks of the Las Orquídeas Member and San Lorenzo Formation, respectively (Table 3). The ε_{Nd} ratios of these arc-rocks range between +6.1 and +7.2 (Table 3).

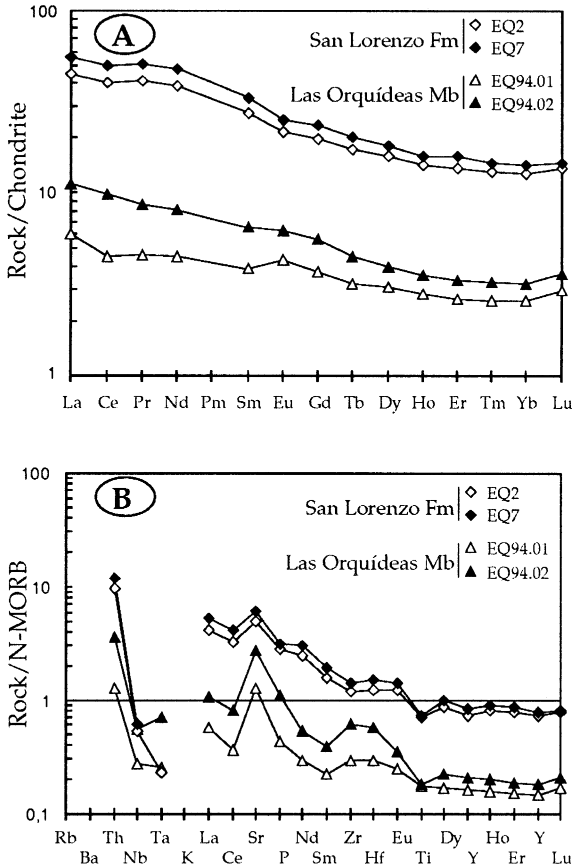

Fig. 10. Chondrite-normalized (Sun and McDonough, 1989) rare earth elements patterns (A) and N-MORB-normalized (Sun and McDonough, 1989) spidergrams (B) of the igneous rocks of the Las Orquídeas Member and San Lorenzo Formation.

The $(^{87}Sr/^{86}Sr)_i$ ratios range between 0.7034 and 0.7046. This large range of $(^{87}Sr/^{86}Sr)_i$ ratios could either reflect hydrothermal alteration or involvement of subducted sediments in the source or fluids released from the hydrothermally altered subducting slab.

6. Comparisons with neighbouring areas and origin of the 'Piñón terrane'

6.1. Comparison between the coast and the Western Cordillera of Ecuador

In the Western Cordillera, the Cretaceous–Palaeogene volcanic and sedimentary rocks are in tectonic contact with the metamorphic basement of the Andean Cordillera. The stratigraphy of these Cretaceous–Palaeogene series (Macuchi Formation s.l., Henderson, 1979, 1981) is still unclear due to a thick Tertiary volcanic cover, and because most of the lithologic units are separated by tectonic contacts (McCourt et al., 1998). The succession of the five main lithologic units may be reconstructed as follows (Faucher et al., 1971; Kehrer and Van der Kaaden, 1979; Cosma et al., 1998).

Tectonic slices of mafic and ultramafic plutonic rocks and pillow basalts are pinched along the contact between the oceanic terranes and the continental margin. On the basis of petrographic and geochemical studies, they were interpreted as belonging to the pre-Late Cretaceous Piñón Formation (Juteau et al., 1977; Lebrat et al., 1987; Desmet, 1994; McCourt et al., 1998). Our data support this interpretation, since trace element and isotopic chemistry show that these rocks represent the deep levels of an oceanic plateau geochemically similar to the Piñón Formation (Cosma et al., 1998; Lapierre et al., 1999). Moreover, a 123 ± 13 Ma Sm/Nd internal isochron obtained from an amphibole-bearing gabbro (Lapierre et al., 1999) is consistent with the stratigraphic data from the Guayaquil area. Therefore, according to the available data, the Piñón Formation of coastal Ecuador is assumed to be of Early Cretaceous age. For this reason, an age of 123 Ma has been used for in-situ decay corrections.

Undated tholeiitic pillow basalts and andesites cropping out in the western part of the Western Cordillera (Toachi beds) were developed in an intra-oceanic arc environment (Cosma et al., 1998). The Toachi beds are interpreted as overlain by greywackes (Pilatón beds) bearing late Turonian to Coniacian inoceramid faunas, which can be correlated with the Cayo Formation of the Guayaquil area (Faucher et al., 1971; Kehrer and Van der Kaaden, 1979). Therefore, the Cretaceous succession of the Western Cordillera is comparable to that of the Guayaquil area of coastal Ecuador (Fig. 2), and the Toachi beds can be correlated with the Las Orquídeas Member of the Guayaquil area, of pre-Cenomanian to pre-Turonian age (Cosma et al., 1998).

The greywackes of the Pilatón beds are locally unconformably overlain by Maastrichtian shales and quartz-rich turbidites of the Yunguilla Formation (Faucher et al., 1971; Bristow and Hoffstetter, 1977; Kehrer and Van der Kaaden, 1979). Although the Yunguilla Formation is coeval with the Guayaquil Formation, the former contains abundant detrital quartz, which is absent in the latter (Fig. 2). This indicates that at least part of the Western Cordillera had been accreted to the continental margin by Maastrichtian times (Faucher et al., 1971; Kehrer and Van der Kaaden, 1979; Lebrat et al., 1987; Cosma et al., 1998). The recent dating of quartz-sandstones as Early to mid-Paleocene in the Western Cordillera supports this interpretation (McCourt et al., 1998). Therefore, the tectonic history of part of the Western Cordillera differs from that of the Guayaquil area, since, by the end of Maastrichtian times, part of the Western Cordillera was already accreted to the continental margin.

Volcaniclastic rocks and calc-alkaline andesites, dacites and breccias (Tandapi beds, Silante Formation) rest unconformably on the Yunguilla Formation. These volcanic rocks are dated by Tertiary radiolarians (Bourgois et al., 1990), scarce K–Ar ages (hornblende) ranging from 51.5 ± 2.5 Ma to 40 ± 3 Ma (Early to Middle Eocene; Wallrabbe-Adams, 1990; Van Thournout et al., 1990), and interbedded limestones and quartz-rich turbidites which yielded Middle to Late Eocene microfossils (Henderson, 1979; Bourgois et al., 1990). Since these volcanic rocks rest on the oceanic terranes of the Western Cordillera and exhibit geochemical features of a continental magmatic arc (Cosma et al., 1998), the accretion of the Western Cordillera was achieved by Early Eocene time (Fig. 2). This interpretation is supported by the fact that the Cretaceous–Palaeogene rocks of the Western Cordillera are unconformably overlain by a sedimentary sequence of Eocene age comparable to that of coastal Ecuador (Bourgois et al., 1990; Jaillard et al., 1995; Fig. 2).

In summary, because of the comparable overlying Cretaceous succession and of their similar geochemical features, we follow the previous workers in admitting that the Piñón Formation of the Guayaquil area correlates with the Early Cretaceous (∼123 Ma) igneous basement of the Western Cordillera, although their tectonic evolution may differ.

6.2. Comparison between western Ecuador and western Colombia

Recent studies carried out in western Colombia distinguish three distinct basaltic suites of oceanic plateau affinities (Fig. 11), i.e. the mafic igneous rocks of the Amaime Formation (>100 Ma), Volcanic Formation (90 Ma), and Serranía de Baudó (78–73 Ma), which successively accreted to the Andean margin (Marriner and Millward, 1984; McCourt et al., 1984; Desmet, 1994; Nivia, 1996; Kerr et al., 1996, 1997b; Sinton et al., 1998).

It appears difficult to correlate the oceanic plateau basement (Piñón Formation and its plutonic roots) of the Western Cordillera and coastal area of Ecuador with the basalts and their plutonic roots of the

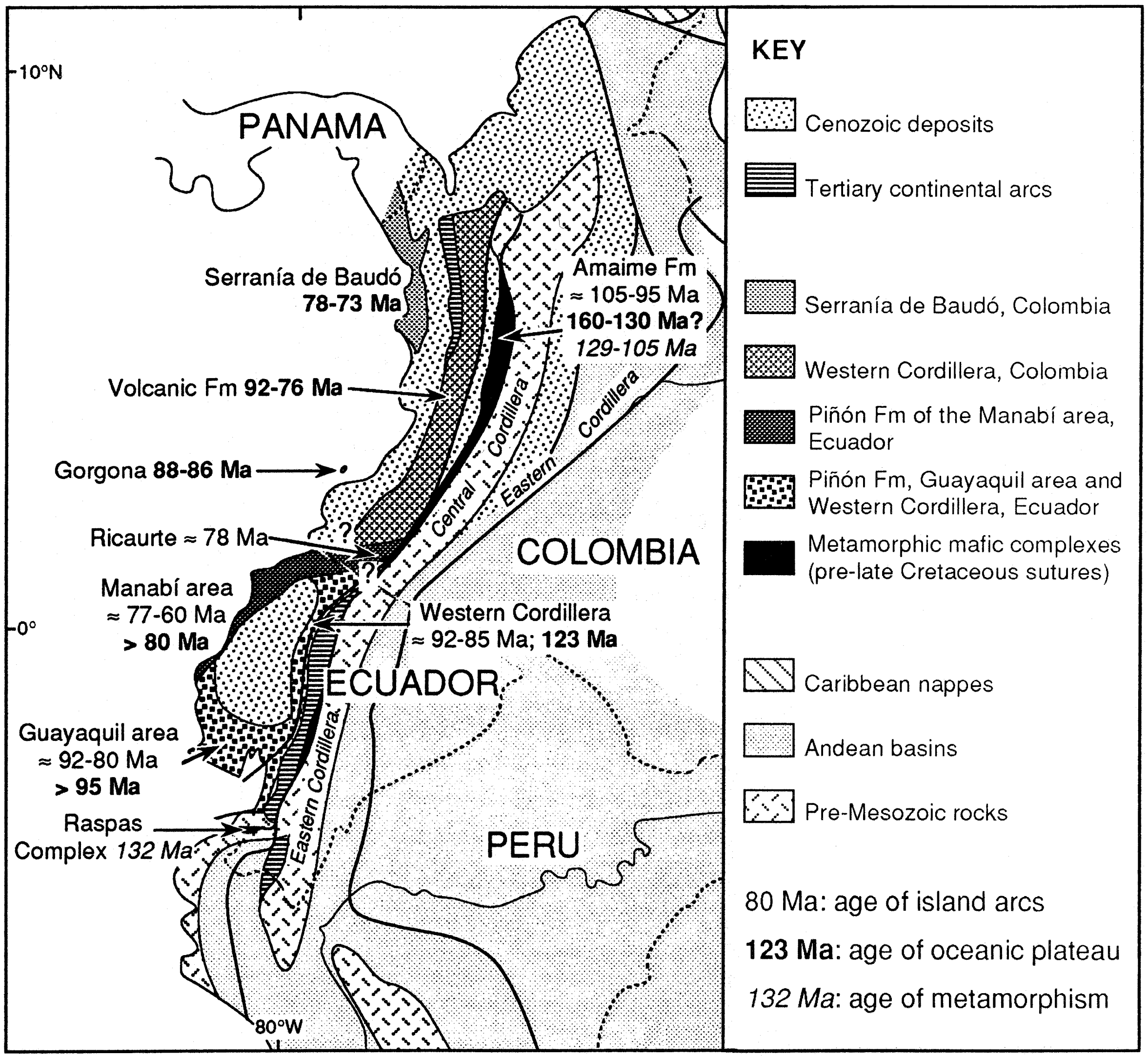

Fig. 11. Schematic geological map of western Colombia and western Ecuador. Numbers indicate the age of oceanic plateaus (bold) and island arcs (standard).

Amaime Formation of Colombia. Indeed, the latter formation is intruded by the Buga batholith dated at 113 ± 10 Ma (K–Ar) and 99 ± 4 Ma (Rb–Sr) (McCourt et al., 1984), indicating that the accretion of the Amaime Formation onto the margin of NW Colombia must have occurred well before 100 Ma (Kerr et al., 1997b). Early Cretaceous ages (129–104 Ma) of high-pressure metamorphic rocks associated with the Amaime Formation are interpreted as reflecting the late stages of accretion, which occurred most probably between 140 and 124 Ma (Aspden and McCourt, 1986; Toussaint and Restrepo, 1994). So the Amaime Formation was probably already accreted while the Piñón Formation of Ecuador erupted. Moreover, in map view, the Western Cordillera of Ecuador is not the continuation of the suture zone of Colombia (Fig. 11). In contrast, the Colombian suture zone is likely correlatable with the Late Jurassic–earliest Cretaceous 'oceanic suture', exposed along the western edge of the Eastern Cordillera of Ecuador (Aspden and Litherland, 1992; Litherland et al., 1994) and/or with the ultramafic and mafic rocks of the Raspas Complex of southwestern Ecuador (Aspden et al., 1995), the high-pressure metamorphism of which has been dated at 132 Ma (K–Ar, Feininger, 1982; Fig. 11).

The age of the oceanic plateau basement of the northwestern area of coastal Ecuador (Manabi area) is pre-late Campanian because intra-oceanic arc lavas and associated pelagic sediments, both of late Campanian–Maastrichtian age, crop out in this area (Lebrat et al., 1987). Thus, this oceanic plateau may be either coeval with the early-Late Cretaceous oceanic plateau generation of western Colombia, or coeval with the Early Cretaceous oceanic plateau of the Guayaquil area and Western Cordillera of Ecuador. More radiometric dates are necessary to distinguish between these two assumptions. The late Campanian–Maastrichtian intra-oceanic arc (San Lorenzo Formation) can be correlated with the Campanian Ricaurte tholeiitic suite of southern Colombia, which seems to have no equivalent farther north (Spadea and Espinosa, 1996; Fig. 11).

Finally, no equivalent of the late-Late Cretaceous (∼78–72 Ma) oceanic plateau of westernmost Colombia (Serranía de Baudó, Kerr et al., 1997b) is known so far in Ecuador.

Therefore, with the possible exception of the northwestern area, the Ecuadorian oceanic plateau terranes are distinct from those accreted to the Colombian margin, and cannot be considered, as a whole, to belong to the Late Cretaceous Colombian–Caribbean Oceanic Plateau as defined by Kerr et al. (1997a).

6.3. A southeastern Pacific origin for the Early Cretaceous terrane of Ecuador

The 123 Ma isochron age suggests that the oceanic plateau of coastal Ecuador is coeval with the southern Pacific large oceanic plateaus generated during the Early Cretaceous 'superplume' (∼125–100 Ma, Larson, 1991), i.e. Kerguelen, Nauru, Manihiki and Ontong Java Plateaus. More specifically, some of the Ecuadorian oceanic plateau fragments are coeval with the early igneous event of the Ontong Java Plateau, recorded at 123 Ma (Mahoney et al., 1993; Coffin and Eldhom, 1993). The overthickened and abnormally buoyant character of the basement of western Ecuador can explain why this oceanic terrane has been accreted to, rather than subducted beneath, the Andean margin (e.g. Cloos, 1993). Moreover, the Piñón Formation forms the basement of distinct and successive Late Cretaceous island arcs, indicating that it behaved as a buoyant upper plate in an intra-oceanic subduction system.

Very little is known about the plate kinematics before the latest Cretaceous. Based on a fixed hotspot reference frame, Duncan and Hargraves (1984) proposed a kinematic reconstruction of the direction and velocity of the northern Farallón and southern Phoenix plates since earliest Cretaceous times. According to this reconstruction, an arbitrary point passively transported by the Farallón plate between 123 and 80 Ma, age of the first accretion of the Piñón terrane to the Andean margin, travelled ∼3500 km northward and more than 3000 km eastward. A point located on the present-day Galápagos 123 Ma ago would be located close to Florida on a 80 Ma reconstructed map. Although uncertainties are great in such a reconstruction, the Early Cretaceous Piñón Formation cannot have been generated by the Galápagos Hotspot, and its source must be located much farther south or southwest.

The Cretaceous migration rates of the Phoenix plate were slower than those of the Farallón plate

(Duncan and Hargraves, 1984) and accordingly, a point colliding the Ecuadorian margin 80 Ma ago must have been located about 2000 km farther south and more than 2500 km to the west, 123 Ma ago. Therefore, if passively transported by the oceanic plate, the Early Cretaceous Piñón Formation must have been generated 3000 to 4000 km southwest of Ecuador on a 80 Ma reconstructed map, that is much closer to the Sala y Gómez Hotspot (Pilger and Handschumacher, 1981) than to the Galápagos Hotspot. However, the presence of pre-Campanian island-arc products (Las Orquídeas Member, Cayo Formation, Toachi and Pilatón beds) indicates that the Piñón Formation has constituted the upper plate of an intra-oceanic subduction system, and has not been transported passively by the oceanic plate during the whole 123–80 Ma time-span. Therefore, the hotspot responsible for the generation of the Piñón Formation may have been located closer to the Ecuadorian margin. A southeastern Pacific origin of the Piñón terrane is consistent with the scarce available palaeomagnetic data, which suggest that coastal Ecuador (taken as a single terrane) originated 5º to the south of its present location (Roperch et al., 1987).

7. Summary and conclusions

(1) Petrographic, mineralogical, chemical and isotopic studies indicate that the basement of western Ecuador is made of oceanic plateau remnants of possibly different ages. Their oceanic plateau origin may explain why these rocks have been accreted to the Andean margin, and why they supported intra-oceanic island arcs.

(2) Three distinct geological domains must be distinguished in western Ecuador. (a) In the northwestern area (Manabí area), the basement is of pre-late Campanian age, an intra-oceanic arc developed in late Campanian–Maastrichtian times, and accretion occurred before the Middle Eocene. (b) In the Central area (Guayaquil area), the basement is of Early Cretaceous age, island arcs were active during the late-Early Cretaceous(?) to early-Late Cretaceous, and the accretion occurred in the Late Paleocene ($\sim$57 Ma). (c) In the Western Cordillera, the basement, preserved as slices in the suture zone, is of Early Cretaceous age ($\sim$123 Ma), intra-oceanic arcs developed during the late-Early Cretaceous(?) to early-Late Cretaceous, and accretion occurred during the Late Cretaceous ($\sim$80 Ma).

(3) No equivalent of the Early Cretaceous oceanic plateau of western Ecuador is thus far known in western Colombia. However, we cannot rule out the possibility that the basement of the northwestern area of coastal Ecuador (Manabí) is coeval to the Caribbean Plateau ($\sim$92–88 Ma). Additionally, remnants of the Late Cretaceous oceanic plateau of westernmost Colombia ($\sim$78–72 Ma) are yet unknown in Ecuador. These observations indicate that most of the oceanic terranes of western Ecuador do not belong to the Colombian–Caribbean Oceanic Plateau. The plume that generated the Early Cretaceous Piñón Plateau must have been located in the southeast Pacific, far south of the present-day Galápagos Hotspot.

Acknowledgements

We are indebted to S. Benítez for his knowledge of the geology of coastal Ecuador and his help in the collection of samples. Field works were supported by the Institut Français de Recherches Scientifiques pour le Développement en Coopération-ORSTOM (presently: Institut de Recherche pour le Développement-IRD), which funded also the analysis, together with the UPRES A 5025 (Grenoble). Thanks are due to the Laboratoire de Géochimie (UMR 5563) of the Université Paul Sabatier of Toulouse (France) for their technical assistance and to the Institut de Minéralogie et de Géologie, Université de Lausanne (Switzerland) for the mineral chemistry. A.C. Kerr and an anonymous reviewer are acknowledged for their constructive and thorough suggestions.

References

Aitken, B.G., Echeverria, L.M., 1984. Petrology and geochemistry of komatiites from Gorgona Island Colombia. Contrib. Mineral. Petrol. 86, 94–105.

Aspden, J.A., Litherland, M., 1992. The geology and Mesozoic collisional history of the Cordillera Real, Ecuador. Tectonophysics 205, 187–204.

Aspden, J.A., McCourt, W.J., 1986. Mesozoic oceanic terrane in the Central Andes of Colombia. Geology 14, 415–418.

Aspden, J.A., McCourt, W.J., Brook, M., 1987. Geometrical control of subduction-related magmatism: the Mesozoic and Cenozoic plutonic history of Western Colombia. J. Geol. Soc., London 144, 893–905.

Aspden, J.A., Bonilla, W., Duque, P., 1995. The El Oro metamorphic complex, Ecuador: geology and economic mineral deposits. Overseas Geol. Miner. Resour. 67, 63 pp., 1 map, BGS publ., Nottingham.

Barrat, J.-A., Keller, F., Amossé, J., Taylor, R.N., Nesbitt, R.W., Hirata, T., 1996. Determination of rare earth elements in sixteen silicate reference samples by ICP–MS using a Tm addition and an ion-exchange chromatography procedure. Geostand. Newsl. 20, 133–139.

Benítez, S., 1995. Evolution géodynamique de la province côtière sud-équatorienne au Crétacé supérieur-Tertiaire. Géol. Alpine 71, 3–163.

Bourgois, J., Egüez, A., Butterlin, J., De Wever, P., 1990. Evolution géodynamique de la Cordillère Occidentale des Andes d'Equateur: la découverte de la formation éocène d'Apagua. C. R. Acad. Sci., Paris (II) 311, 173–180.

Bristow, C.R., Hoffstetter, R., 1977. Ecuador. Lexique Stratigraphique International, Vol. 5a2, CNRS, Paris, 410 pp.

Castillo, P., Batiza, R., Stern, R.J., 1986. Petrology and geochemistry of Nauru Basin igneous complex: large volume, off-ridge eruptions of MORB-like basalt during the Cretaceous. Init. Rep. DSDP 89, 555–576.

Cloos, M., 1993. Lithospheric buoyancy and collisional orogenesis: subduction of oceanic plateaus, continental margins, island arcs, spreading ridges, and seamounts. Geol. Soc. Am. Bull. 105, 715–737.

Coffin, M.F., Eldhom, O., 1993. Scratching the surface: estimating dimension of Large Igneous Provinces. Geology 21, 515–518.

Cosma, L., Lapierre, H., Jaillard, É., Laubacher, G., Bosch, D., Desmet, A., Mamberti, M., Gabriele, P., 1998. Pétrographie et géochimie de la Cordillère Occidentale du Nord de l'Équateur (0º30′S): implications tectoniques. Bull. Soc. Géol. Fr. 169, 739–751.

Daly, M.C., 1989. Correlations between Nazca/Farallón plate kinematics and Forearc basin evolution in Ecuador. Tectonics 8, 769–790.

Desmet, A., 1994. Ophiolites et séries basaltiques crétacées des régions caraïbes et norandines: bassins marginaux, dorsales ou plateaux océaniques? Doct. Thesis, Univ. Nancy 1, 589 pp.

Doe, B.R., 1970. Lead Isotopes. Springer, New York, 137 pp.

Duncan, R.A., Hargraves, R.B., 1984. Plate tectonic evolution of the Caribbean region in the mantle reference frame. Geol. Soc. Am. Mem. 162, 81–93.

Dupré, B., Echeverria, L.M., 1984. Pb isotopes of Gorgona island (Colombia): isotope variations correlated with magma type. Earth Planet. Sci. Lett. 67, 186–190.

Faucher, B., Vernet, R., Bizon, G., Bizon, J.J., Grekoff, N., Lys, M., Sigal, J., 1971. Sedimentary Formations in Ecuador. A stratigraphic and micropaleontological survey. Bureau Études Indust. Coop. Inst. Fr. Pétrole (BEICIP), 220 pp., 3 Vols.

Feininger, T., 1982. The metamorphic 'basement' of Ecuador. Geol. Soc. Am. Bull. 93, 87–92.

Feininger, T., Bristow, C.R., 1980. Cretaceous and Paleogene history of coastal Ecuador. Geol. Rundsch. 69, 849–874.

Gansser, A., 1973. Facts and theories on the Andes. J. Geol. Soc., London 129, 93–131.

Goossens, P.J., Rose, W.I., 1973. Chemical composition and age determination of tholeiitic rocks in the basic Cretaceous Complex, Ecuador. Geol. Soc. Am. Bull. 84, 1043–1052.

Goossens, P.J., Rose, W.I., Flores, D., 1977. Geochemistry of tholeiites of the Basic Igneous Complex of Northwestern South America. Geol. Soc. Am. Bull. 88, 1711–1720.

Haq, B.U., Van Eysinga, F.W.B., 1998. Geological Time Table (5th ed.). Elsevier, Amsterdam.

Hart, S.R., 1984. A large-scale isotope anomaly in the Southern Hemisphere mantle. Nature 309, 753–757.

Hauff, F., Hoernle, K., Schminke, H.-U., Werner, R., 1997. A mid-Cretaceous origin for the Galápagos Hotspot: volcanological, petrological and geochemical evidence from Costa Rican oceanic crustal fragments. Geol. Rundsch. 86, 141–155.

Henderson, W.G., 1979. Cretaceous to Eocene volcanic arc activity in the Andes of northern Ecuador. J. Geol. Soc., London 136, 367–378.

Henderson, W.G., 1981. The volcanic Macuchi Formation. Andes of Northern Ecuador. Newslett. Stratigr. 9, 157–168.

Hofmann, A.W., 1988. Chemical differentiation of the Earth: the relationship between mantle, continental crust, and oceanic crust. Earth Planet. Sci. Lett. 90, 297–314.

Jaillard, É., Soler, P., Carlier, G., Mourier, T., 1990. Geodynamic evolution of the northern and central Andes during early to middle Mesozoic times: a Tethyan model. J. Geol. Soc., London 147, 1009–1022.

Jaillard, É., Ordoñez, M., Benítez, S., Berrones, G., Jiménez, N., Montenegro, G., Zambrano, I., 1995. Basin development in an accretionary, oceanic-floored forearc setting: southern coastal Ecuador during late Cretaceous to late Eocene times. In: Tankard, A.J., Suárez, R., Welsink, H.J. (Eds.), Petroleum Basins of South America. Am. Assoc. Pet. Geol. Mem. 62, 615–631.

Jaillard, É., Benítez, S., Mascle, G., 1997. Les déformations paléogènes de la zone d'avant-arc sud-équatorienne en relation avec l'évolution géodynamique. Bull. Soc. Géol. Fr. 168, 403–412.

James, D.E., 1971. Plate tectonic model for the evolution of the Central Andes. Geol. Soc. Am. Bull. 82, 3325–3346.

Juteau, T., Mégard, F., Raharison, L., Whitechurch, H., 1977. Les assemblages ophiolitiques de l'Occident équatorien: nature pétrographique et position structurale. Bull. Soc. Géol. Fr. (7) 19, 1127–1132.

Kehrer, W., Van der Kaaden, G., 1979. Notes on the geology of Ecuador with special reference to the Western Cordillera. Geol. Jahrb. B 35, 5–57.

Kerr, A.C., Tarney, J., Marriner, G.F., Nivia, A., Klaver, G.Th., Saunders, A.D., 1996. The geochemistry and tectonic setting of Late Cretaceous Caribbean and Colombian volcanism. J. S. Am. Earth Sci. 9, 111–120.

Kerr, A.C., Tarney, J., Marriner, G.F., Nivia, A., Saunders, A.D., 1997a. The Caribbean–Colombian Cretaceous igneous province: the internal anatomy of an oceanic plateau. In: Mahoney, J.J., Coffin, M.F. (Eds.), Large Igneous Provinces: Continental, Oceanic and Planetary Flood Volcanism. Am. Geophys. Union Monogr. 100, 123–144.

Kerr, A.C., Marriner, G.F., Tarney, J., Nivia, A., Saunders, A.D., Thirlwall, M.F., Sinton, C., 1997b. Cretaceous basaltic terranes in Western Colombia: elemental, chronological and Sr–Nd isotopic constraints on petrogenesis. J. Petrol. 38, 677–702.

Lapierre, H., Dupuis, V., Mercier de Lépinay, B., Tardy, M., Ruíz, J., Maury, R.C., Hernandez, J., Loubet, M., 1997. Is the Lower Duarte Igneous Complex (Hispaniola) a remnant of the Caribbean plume-generated oceanic plateau? J. Geol. 105, 111–120.

Lapierre, H., Dupuis, V., Bosch, D., Polvé, M., Maury, R.C., Hernandez, J., Monié, P., Yéghicheyan, D., Jaillard, É., Tardy, M., Mercier de Lépinay, B., Mamberti, M., Desmet, A., Keller, F., Sénebier, F., 1999. Multiple plume events in the genesis of the peri-Caribbean Cretaceous Oceanic Plateau Province. J. Geophys. Res. (in press).

Larson, R.L., 1991. Geological consequences of superplumes. Geology 19, 961–966.

Lebrat, M., Mégard, F., Dupuy, C., Dostal, J., 1987. Geochemistry and tectonic setting of pre-collision Cretaceous and Paleogene volcanic rocks of Ecuador. Geol. Soc. Am. Bull. 99, 569–578.

Leterrier, J., Maury, R.C., Thonon, P., Girard, D., Marchal, M., 1982. Clinopyroxene composition as a method of identification of magmatic affinities of paleo-volcanic series. Earth Planet. Sci. Lett. 59, 139–154.

Litherland, M., Aspden, J.A., Jemielita, R.A., 1994. The metamorphic belts of Ecuador. Br. Geol. Surv., Overseas Mem. 11, 147 pp., 2 maps.

Mahoney, J.J., Storey, M., Duncan, R.A., Spencer, K.J., Pringle, M., 1993. Geochemistry and age of the Ontong Java Plateau. In: Pringle, M.S., Sager, W.W., Sliter, W.V., Stein, S. (Eds.), The Mesozoic Pacific: Geology, Tectonics and Volcanism. Geophys. Monogr. 77, 233–261.

Manhès, G., Allègre, C.J., Dupré, B., Hamelin, B., 1980. Lead isotope study of basic–ultrabasic layered complex: speculations about the ages of the Earth and primitive mantle characteristics. Earth Planet. Sci. Lett. 43, 370–382.

Marriner, G.F., Millward, D., 1984. The petrology and geochemistry of Cretaceous to Recent volcanism in Colombia: the magmatic history of an accretionary plate margin. J. Geol. Soc., London 141, 473–486.

McCourt, W.J., Aspden, J.A., Brook, M., 1984. New geological and geochronological data from the Colombian Andes: continental growth by multiple accretion. J. Geol. Soc., London 141, 831–845.

McCourt, W.J., Duque, P., Pilatasig, L.F., Villagómez, R., 1998. Mapa geológico de la Cordillera Occidental del Ecuador entre 1º–2ºS., escala 1/200.000. CODIGEM-Min. Energ. Min. – BGS publs., Quito.

Mégard, F., 1987. Cordilleran and marginal Andes: a review of Andean geology North of the Arica elbow (18ºS). In: Monger, J.W.H., Francheteau, J. (Eds.), Circum-Pacific Orogenic Belts and Evolution of the Pacific Ocean Basin. Geodyn. Ser. 18, 71–95.

Millward, D., Marriner, G.F., Saunders, A.D., 1984. Cretaceous tholeiitic volcanic rocks from the Western Cordillera of Colombia. J. Geol. Soc., London 141, 847–860.

Morimoto, M., 1988. Nomenclature of pyroxenes. Miner. Mag. 52, 535–550.

Nivia, A., 1996. The Bolivar mafic–ultramafic complex, SW Colombia: the base of an obducted oceanic plateau. J. S. Am. Earth Sci. 9, 59–68.

Ordoñez, M., 1996. Aplicaciones del estudio de microfósiles en la industria petrolera ecuatoriana. Actas VII Congr. Ecuat. Geol. Min. Petrol., Quito, pp. 38–52.

Pichler, H., Aly, S., 1983. Neue K–Ar Alter plutonischer Gesteine in Ecuador. Zeitbl. dtsch. Geol. Ges. 134, 495–506.

Pilger, R.H., Handschumacher, D.W., 1981. The fixed hotspot hypothesis and origin of the Easter-Sala y Gomez-Nazca trace. Bull. Geol. Soc. Am. 92, 437–446.

Roperch, P., Mégard, F., Laj, C., Mourier, T., Clube, T., Noblet, C., 1987. Rotated oceanic blocks in Western Ecuador. Geophys. Res. Lett. 14, 558–561.

Sen, G., Hickey-Vargas, R., Waggoner, D.G., Maurasse, F., 1988. Geochemistry of basalts from the Dumisseau Formation, southern Haiti: implications for the origin of the Caribbean Sea crust. Earth Planet. Sci. Lett. 87, 423–437.

Sigal, J., 1969. Quelques acquisitions récentes concernant la chrono-stratigraphie des formations sédimentaires de l'Équateur. Rev. Esp. Micropaleontol. 1, 205–236.

Sinclair, J.H., Berkey, C.P., 1924. Geology of Guayaquil, Ecuador, South America. Am. J. Sci. 7 (42), 491–497.

Sinton, C.W., Duncan, R.A., Denyer, P., 1997. Nicoya Peninsula, Costa Rica: a single suite of Caribbean oceanic plateau magmas. J. Geophys. Res. 102, 15507–15520.

Sinton, C.W., Duncan, R.A., Storey, M., Lewis, J., Estrada, J.J., 1998. An oceanic flood basalt province within the Caribbean plate. Earth Planet. Sci. Lett. 155, 221–235.

Spadea, P., Espinosa, A., 1996. Petrology of late Cretaceous volcanic rocks from the southernmost segment of the Western Cordillera of Colombia (South America). J. S. Am. Earth Sci. 9, 79–90.

Sun, S.S., McDonough, W.F., 1989. Chemical and isotopic systematics of oceanic basalts. In: Saunders, A.D., Norry, M.J. (Eds.), Magmatism in the Ocean Basins. Geol. Soc. Spec. Publ. 42, 313–345.

Thalmann, H.E., 1946. Micropaleontology of Upper Cretaceous and Paleocene in Western Ecuador. Am. Assoc. Pet. Geol. Bull. 30, 337–347.

Toussaint, J.-F., Restrepo, J.J., 1994. The Colombian Andes during Cretaceous times. In: Salfity, J.A. (Ed.), Cretaceous Tectonics in the Andes. Earth Evol. Sci., Vieweg, Braunschweig, pp. 61–100.

Van Thournout, F., Quevedo, L., Pasteels, P., Boven, A., 1990. Radiometric ages of igneous rocks from Northwestern Ecuador. Bull. Soc. Belge Géol. 99, 71–77.

Van Thournout, F., Hertogen, J., Quevedo, L., 1992. Allochthonous terranes in northwestern Ecuador. Tectonophysics 205, 205–221.

Wallrabbe-Adams, H.-J., 1990. Petrology and geotectonic development of the Western Ecuadorian Andes: the Basic Igneous Complex. Tectonophysics 185, 163–182.

Wasserburg, G.J., Jacobsen, S.B., DePaolo, D.J., McCulloch, M.T., Wen, T., 1981. Precise determination in Sm/Nd ratios, Sm and Nd isotopic abundance in standard solutions. Geochim. Cosmochim. Acta 45, 2311–2323.

White, W.M., Hofmann, A.W., Puchelt, H., 1987. Isotope geochemistry of Pacific mid-ocean ridge basalt. J. Geophys. Res. 92, 4881–4893.

White, W.M., McBirney, A.R., Duncan, R.A., 1993. Petrology and geochemistry of the Galápagos islands: portrait of a pathological mantle plume. J. Geophys. Res. 98, 19533–19563.